

## Mass measurements of the proton-rich nuclei $^{50}\text{Fe}$ and $^{54}\text{Ni}^\dagger$

R. E. Tribble,\* J. D. Cossairt, D. P. May, and R. A. Kenefick

Cyclotron Institute and Physics Department, Texas A & M University, College Station, Texas 77843

(Received 6 December 1976)

The reactions  $^{54}\text{Fe}(^4\text{He}, ^8\text{He})^{50}\text{Fe}$  and  $^{58}\text{Ni}(^4\text{He}, ^8\text{He})^{54}\text{Ni}$  have been observed at an incident  $\alpha$  energy of 110 MeV. The reaction  $Q$  values are found to be  $Q(^{50}\text{Fe}) = -50.95 \pm 0.06$  MeV and  $Q(^{54}\text{Ni}) = -50.19 \pm 0.05$  MeV. The experiments provide the first observation and subsequent mass measurement of the proton-rich nuclei  $^{50}\text{Fe}$  and  $^{54}\text{Ni}$ .

[NUCLEAR REACTIONS  $^{54}\text{Fe}(^4\text{He}, ^8\text{He})$  and  $^{54}\text{Ni}(^4\text{He}, ^8\text{He})$ . Measured reaction  $Q$  values and mass excesses of  $^{50}\text{Fe}$  and  $^{54}\text{Ni}$ .]

The ( $^4\text{He}, ^8\text{He}$ ) reaction has proven to be quite useful for obtaining masses of proton-rich nuclei. To date, such mass measurements have been confined to  $T_z = -2$  nuclei with  $A < 40$ .<sup>1-4</sup> We report here the first observation and consequent mass measurement of the  $T_z = -1$  nuclei  $^{50}\text{Fe}$  and  $^{54}\text{Ni}$  via the  $^{54}\text{Fe}(^4\text{He}, ^8\text{He})^{50}\text{Fe}$  and  $^{58}\text{Ni}(^4\text{He}, ^8\text{He})^{54}\text{Ni}$  reactions. These masses extend our knowledge of proton-rich nuclei in the  $f_{7/2}$  shell and provide direct tests of the mass formulas used to predict the proton-rich limit of  $\beta$  stability. These masses also allow a determination of the  $T = 1$  Coulomb energies in both  $A = 50$  and  $A = 54$ .

The experiments were performed with energy analyzed beams of 110-MeV  $\alpha$  particles from the Texas A & M University 88-inch cyclotron.  $^8\text{He}$  spectra were obtained in the focal plane of an Enge split-pole magnetic spectrograph at a laboratory scattering angle of  $5^\circ$ . The focal plane detector consisted of a 10-cm single-wire gas proportional counter backed by a 5-cm  $\times$  1-cm  $\times$  600- $\mu\text{m}$  Si solid-state detector. Particle identification was performed by the three constraints (1)  $(dE/dx)_{\text{gas}}$ , (2)  $E_{\text{Si}}$ , and (3) time of flight relative to the cyclotron rf signal. Particle position was obtained by charge division performed by an on-line computer. Pile-up rejection was used in conjunction with the solid-state detector so that relatively high count rates could be achieved without significant loss of resolution. This detector system has proven to be quite sensitive for low cross section experiments (see e.g., Ref. 2), especially when the  $^8\text{He}$  particles are stopped in the solid-state detector. Thus 0.125 mm of Kapton foil was inserted as a degrader between the gas counter and the Si detector to ensure that the  $^8\text{He}$ 's would stop.

The Fe and Ni targets were nominally 2-mg/cm<sup>2</sup> rolled foils, isotopically enriched to 96.7%  $^{54}\text{Fe}$  and 99.9%  $^{58}\text{Ni}$ , respectively. Actual target thicknesses were obtained by weighing and by  $^{241}\text{Am}$   $\alpha$  energy loss measurements, which agreed to

about 10%. The  $\alpha$  energy loss was determined both before and after the experiments in order to check for any change in the target composition due to surface contamination.

The incident beam energy was determined via the momentum matching technique<sup>5</sup> by using an  $H_2^+$  beam of the same magnetic rigidity as the incident  $\alpha$  beam. Reaction products from  $^{16}\text{O}(p, p)$   $^{16}\text{O}(g.s.)$  and  $^{16}\text{O}(p, d)$   $^{15}\text{O}(g.s.)$  were observed simultaneously at a laboratory scattering angle of  $20^\circ$ . Thus the  $H_2^+$  beam was measured and correspondingly the incident  $\alpha$  beam energy was determined to an uncertainty of 20 keV.

$\alpha$  elastic scattering from either the  $^{54}\text{Fe}$  or  $^{58}\text{Ni}$  target provided an initial focal plane calibration. The  $^8\text{He}$  magnetic rigidity was higher than that for elastic  $\alpha$  particles, thus requiring a 4% magnetic field shift. As an additional calibration, spectra from  $^{54}\text{Fe}(^4\text{He}, ^6\text{He})^{52}\text{Fe}$  and  $^{58}\text{Ni}(^4\text{He}, ^6\text{He})^{56}\text{Ni}$  were obtained simultaneously with the  $^8\text{He}$  spectra. Although the  $^6\text{He}$  energy corresponded to an excitation of  $\sim 8$  MeV in  $^{52}\text{Fe}$  and  $^{56}\text{Ni}$ , the spectra did show definite structure. In a separate experiment [but performed under the same conditions as the original ( $^4\text{He}, ^8\text{He}$ ) reactions] the structures, which could likely consist of multiple peak excitations, were calibrated against the  $^{12}\text{C}(^4\text{He}, ^6\text{He})^{10}\text{C}(g.s.)$  and  $^{24}\text{Mg}(^4\text{He}, ^6\text{He})^{22}\text{Mg}(E_x = 1.25, 3.31 \text{ MeV})$  reactions. During this calibration, the spectrograph angle was checked by observing  $^{12}\text{C}(^4\text{He}, ^4\text{He}')^{12}\text{C}(E_x = 4.44 \text{ MeV})$  and  $p(^4\text{He}, ^4\text{He})p$  simultaneously from a Formvar target. The angle determination removed the calibration uncertainty due to different kinematic shifts for the  $^6\text{He}$ 's from the light ( $A = 12$ ) and heavy ( $A = 54, 58$ ) mass targets. Calibrated  $^6\text{He}$  spectra from  $^{54}\text{Fe}$  and  $^{58}\text{Ni}$  are shown in Fig. 1.

From previous ( $^4\text{He}, ^8\text{He}$ ) measurements, the cross sections to  $^{50}\text{Fe}$  and  $^{54}\text{Ni}$  were expected to be quite low. Therefore, the experiments were optimized to obtain enough events to be identi-

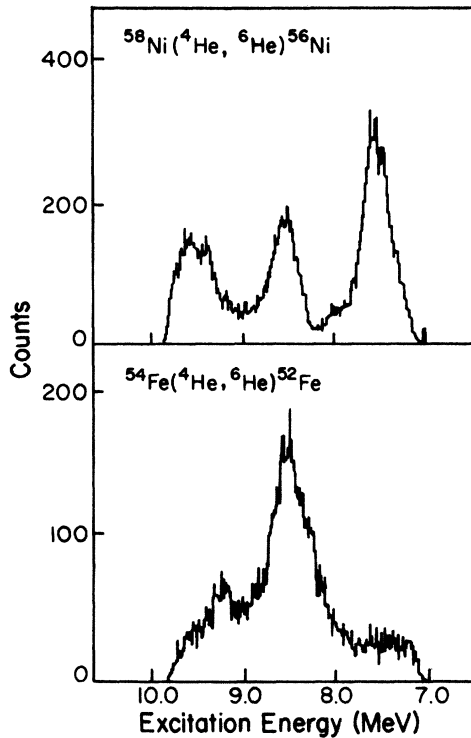


FIG. 1.  ${}^6\text{He}$  spectra obtained at the  ${}^8\text{He}$  magnetic field.

fiable as a peak in a 48-h experiment. Beam currents on target were typically  $1.5 \mu\text{A}$ , with  $<5\%$  pulse pile-up rejection losses. The spectrograph was operated with a 2.3-msr solid angle corresponding to an integration from  $3.5^\circ$  to  $6.5^\circ$  in  $\theta$ . The target thicknesses were chosen to provide sensitivities to peak cross sections  $< \frac{1}{4}$  nb/sr.

The resulting  ${}^8\text{He}$  spectra are shown in Fig. 2. We assume that the peaks in the two spectra are due to the  ${}^{54}\text{Fe}$  and  ${}^{58}\text{Ni}$  ( ${}^4\text{He}$ ,  ${}^8\text{He}$ ) reactions. Background due to light contaminants such as  ${}^{12}\text{C}$  and  ${}^{16}\text{O}$  can be eliminated because their ground state  $Q$  values are more negative than the  ${}^{54}\text{Fe}$  and  ${}^{58}\text{Ni}$   $Q$  values. Other Fe and Ni isotopes could produce background, however. In the Fe spectrum there are such background events that we attribute to the 3.3% of other Fe isotopes. It is unlikely that the peaks are background since they would represent large (15–20 nb/sr) cross sections to discrete states in the continuum.

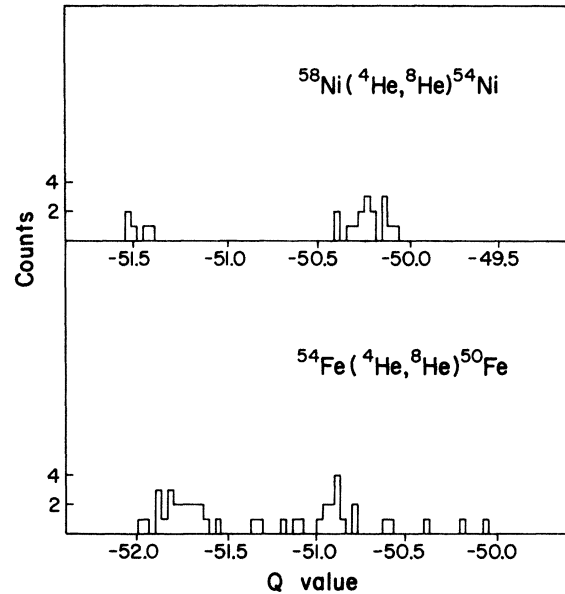


FIG. 2.  ${}^8\text{He}$  spectra as a function of  $Q$  value.

Laboratory cross sections for the  ${}^{50}\text{Fe}$  and  ${}^{54}\text{Ni}$  ground states, averaged over the spectrograph solid angle, are  $\sim \frac{1}{2}$  nb/sr at  $\theta_{\text{lab}} = 5^\circ$ , with up to 50% uncertainties due to statistics, beam integration, and vertical efficiency in the spectrograph focal plane.

Beam energy, focal plane calibration, scattering angle, and target thicknesses determined the  $Q$ -value scales shown in Fig. 2. The resulting  $Q$  values and mass excesses (all in MeV) are  $Q({}^{50}\text{Fe}) = -50.95 \pm 0.06$ ,  $M({}^{50}\text{Fe}) = -34.48 \pm 0.06$  and  $Q({}^{54}\text{Ni}) = -50.19 \pm 0.05$ ,  $M({}^{54}\text{Ni}) = -39.21 \pm 0.05$ , with the mass results based on a  ${}^8\text{He}$  mass excess of  $31.601 \pm 0.013$  MeV.<sup>6</sup> Mass uncertainties are dominated by centroid statistical uncertainty in both cases, although background in the  ${}^{50}\text{Fe}$  spectrum contributes an additional uncertainty in that mass determination. The centroid uncertainties, including background, are 35-keV  ${}^{54}\text{Ni}$  and 50-keV  ${}^{50}\text{Fe}$ . The other significant uncertainties are the  ${}^8\text{He}$  mass—13 keV, and the focal plane calibration—18 keV. Uncertainties associated with target thickness, beam energy, and scattering angle are

TABLE I. Properties of  ${}^{50}\text{Fe}$  and  ${}^{54}\text{Ni}$ . All entries are in MeV.

Nuclide	Expt.	Mass excess		$S_{1p}$	$S_{2p}$	Coulomb energy
		Garvey and Kelson <sup>a</sup>	Coulomb energy <sup>b</sup>			
${}^{50}\text{Fe}$	$-34.48 \pm 0.06$	-34.50	$-34.472 \pm 0.013$	4.16	6.24	$8.93 \pm 0.06$
${}^{54}\text{Ni}$	$-39.21 \pm 0.05$	-39.27	$-39.296 \pm 0.013$	3.85	5.46	$9.58 \pm 0.05$

<sup>a</sup>Reference 7.

<sup>b</sup>Reference 8.

small since either the  $^{54}\text{Fe}(^4\text{He}, ^6\text{He})^{52}\text{Fe}$  or  $^{58}\text{Ni}(^4\text{He}, ^6\text{He})^{56}\text{Ni}$  reactions are used to calibrate the focal plane. The spectra in Fig. 2 indicate possible excited states in both nuclei, but an apparent excited state in  $^{54}\text{Ni}$  is cut off by the edge of the detector active region. In  $^{50}\text{Fe}$  we definitely observe an excited state at  $E_x = 0.81 \pm 0.08$  MeV ( $Q = -51.00 \pm 0.06$  MeV).

The new masses are compared with the symmetric Garvey-Kelson mass predictions<sup>7</sup> and a recent Coulomb energy prediction<sup>8</sup> in Table I. In both cases the predictions are nearly the same and are in good agreement with the experimental results. Also included in the table are the  $T=1$  Coulomb energies. These new results are based on  $T=1$  assignments for the ground states of the  $T_z=0$  nuclei  $^{50}\text{Mn}$  and  $^{54}\text{Co}$ .<sup>9</sup> Finally, the separa-

tion energies for 1 and 2 proton decays are included in the table to show that both nuclei are particle stable.

The new masses allow for reasonable estimates of the  $\beta$  decay properties of  $^{50}\text{Fe}$  and  $^{54}\text{Ni}$ . The end point energies for the positron decays are  $E_0(^{50}\text{Fe}) = 7.12 \pm 0.06$  MeV and  $E_0(^{54}\text{Ni}) = 7.77 \pm 0.05$  MeV. These energies are somewhat greater than the proton separation energies in  $^{50}\text{Mn}$  (4.53 MeV) and  $^{54}\text{Co}$  (4.36 MeV) and hence both  $^{50}\text{Fe}$  and  $^{54}\text{Ni}$  could be delayed proton emitters. However, such decays would not be competitive with the fast superallowed  $0^+ \rightarrow 0^+$   $\beta$  transition. Assuming 100% branching ratios for the superallowed decays, and also an  $ft$  of 3090 sec,<sup>9</sup> the predicted half-lives would be  $t_{1/2}(^{50}\text{Fe}) = 200$  ms and  $t_{1/2}(^{54}\text{Ni}) = 140$  ms.

†Supported in part by the National Science Foundation.

\*Alfred P. Sloan Fellow.

<sup>1</sup>R. G. H. Robertson, S. Martin, W. R. Falk, D. Ingham, and A. Djalois, *Phys. Rev. Lett.* **32**, 1207 (1974).

<sup>2</sup>R. E. Tribble, R. A. Kenefick, and R. L. Spross, *Phys. Rev. C* **13**, 50 (1976).

<sup>3</sup>R. E. Tribble, J. D. Cossairt, and R. A. Kenefick, *Phys. Lett.* **61B**, 353 (1976).

<sup>4</sup>R. E. Tribble, J. D. Cossairt, and R. A. Kenefick (unpublished).

<sup>5</sup>G. F. Trentelman and E. Kashy, *Nucl. Instrum. Methods* **82**, 304 (1970).

<sup>6</sup>R. Kouzes and W. H. Moore, *Phys. Rev. C* **12**, 1511

(1975); J. W. Jäneke, F. D. Becchetti, L. Chua, and A. Vander Molen, *ibid.* **11**, 2114 (1975); J. Cerny, N. A. Jelley, D. L. Hendrie, C. F. Maguire, J. Mahoney, D. K. Scott, and R. B. Weisenmiller, *ibid.* **10**, 2654 (1974).

<sup>7</sup>D. Mueller, E. Kashy, W. Benenson, and H. Nann, *Phys. Rev. C* **12**, 51 (1975); E. Kashy, private communication.

<sup>8</sup>R. Sherr, private communication (unpublished).

<sup>9</sup>J. C. Hardy, G. C. Ball, J. S. Geiger, R. L. Graham, J. A. Macdonald, and H. Schmeing, *Phys. Rev. Lett.* **33**, 320 (1974).